Construction and Building Materials 34 (2012) 372–380

Contents lists available at SciVerse ScienceDirect

Construction and Building Materials

journal homepage: www.elsevier.com/locate/conbuildmat

Tensile characterization of basalt fiber rods and ropes: A first contribution

Enrico Quagliarini [a,*], Francesco Monni [a], Stefano Lenci [a], Federica Bondioli [b]

[a] Department of Architecture, Building and Civil Engineering, Polytechnic University of Marche, via Brecce Bianche, 60131 Ancona, Italy
[b] Department of Materials and Environmental Engineering, University of Modena and Reggio Emilia, via Vignolese 905, 41125 Modena, Italy

ARTICLE INFO

Article history:
Received 3 October 2011
Received in revised form 13 January 2012
Accepted 25 February 2012

Keywords:
Basalt fiber rope
Basalt fiber rod
Tensile test

ABSTRACT

Basalt is an emerging material, whose use is increasing in constructions and civil applications as an alternative to glass, carbon or aramidic fibers. Basalt Fiber Reinforced Polymer (BFRP) rods and Basalt Fiber (BF) ropes are going to be used as an alternative to glass, carbon or aramidic fibers for strengthening purposes but few information about their mechanical performances is present in literature and standard test protocols are missing. Thus, this work tries to provide a test protocol for tensile characterization of BF ropes and a validation of the test protocol used for tensile characterization of not-basalt-FRP rods applied on BFRP rods. This is a very important issue from an engineering standpoint in order to evaluate their applicability for architectural heritage retrofitting, as, for example, in repointing (rods), or in innovative techniques, such as the one actually still being tested in our laboratories, that is aimed to strengthen historic masonry (ropes). Experimental test results obtained are shown. Results seem to confirm that BFRP rods and BF ropes could be a good alternative to other similar products.

1. Introduction

Basalt is a natural material that is found in volcanic rocks originated from frozen lava. Since antiquity basalt is used (as crushed rock) in construction and Romans recognized its strength and durability using it in road construction as flagstone. Basalt rocks can be molten approximately between 1500 and 1700 °C [1,2]. After the Second World War, the use of basalt fibers became topics of ex USSR defense and aerospace applications research programs, from that emerging the idea of using basalt fibers as reinforcement of composite materials [3]. Also today continuous basalt fibers are mainly manufactured in USA, China and East Europe countries [4]. Continuous basalt fibers are obtained by melting basalt and forcing it through in platinum/rhodium crucible bushings to create fibers [5]. This technology (continuous spinning) can offer the reinforcement material in the form of chopped fibers or continuous fibers, that can be used in the textile field manufacturing process and have a great potential application to composite materials [2,6]. Beyond having ability to be easily processed using conventional processes and equipments, in addition, the basalt fibers do not contain any other additives in a single producing process. This makes them have an additional advantage in cost: this kind of fibers is considered less expensive than the glass ones, the most similar to them [2,6,7]. Other advantages like high modulus, heat resistance, heat and sound insulating properties, good resistance to chemical attack and in seawater environment [8], make basalt fibers a good alternative to glass fibers as reinforcing material in composites used in several fields such as marine [9], automotive, sporting equipment [10]. In construction field, basalt is proposed in form of short fibers for insulating material (basalt wool), for reinforced concrete (chopped fibers) or like reinforcing material in restoration and rehabilitation of concrete [11] and masonry structures [12], or like reinforcing material for Fiber Reinforced Polymer (FRP) bars used in concrete technology [13]. It is also important the application in passive fire protection field [14]. Basalt fibers have a good resistance to weather, alkaline and acids exposure; basalt fibers can be used from −200 °C to 600–800 °C [1,6,7,11,15]. As shown in [16] even if asbestos and basalt fibers present similar composition, basalt seems to be safe, because of different morphology and surface properties avoid any carcinogenic or toxicity effects, which are presented by asbestos instead. For all of these reasons, basalt fibers products can be considered attractive in many industrial fields, like constructions and civil structures, but they are still not so known. So it is necessary to have as soon as possible experimental results about mechanical properties of basalt fibers products in order to show their performance and evaluate their applicability. This work focuses on tensile characterization of basalt FRP rods and Basalt Fiber (BF) ropes. Several studies have shown the efficacy of FRP rods in construction field as reinforcement for strengthening and restoration of building heritage. As an example, the use of reinforcing rods in masonry mortar joints, called "repointing" has been proposed for strengthening masonry structures. It can be performed using steel [17] or FRP rods [18]. As regards BF ropes, it is a new product with no specific use at the moment in constructions and civil

* Corresponding author. Tel.: +39 0712204248; fax: +39 0712204378.
E-mail address: e.quagliarini@univpm.it (E. Quagliarini).

0950-0618/$ - see front matter © 2012 Elsevier Ltd. All rights reserved.
doi:10.1016/j.conbuildmat.2012.02.080

applications but it looks like a very promising one when employed in an innovative technique, actually still being tested in our laboratories, aimed to strengthen historic masonry creating an embracing reinforcing mesh.

In this way, this paper tries to provide a validation of the test protocol used for tensile characterization of GFRP rods without continuous embossed rib [19,20] applied on BFRP rods with continuous embossed rib. Moreover, a test protocol for tensile characterization of BF ropes is presented in order to evaluate their possible employment in existing masonry strengthening. Finally, test results obtained on BFRP rods and BF ropes are shown: in fact, it is necessary to have a full characterization of the mechanical properties of these products, to be aware of effective performance shown by them, for a sure employment in constructions, not only for design purposes but also for quality control and optimization purposes by manufacturers.

2. Materials and methods

2.1. BFRP rods

2.1.1. Main features

The material used in this experimental work is an FRP rod manufactured using continuous basalt fibers. In Table 1 the only information provided by manufacturer about the fiber used is reported. The most interesting feature of this kind of product is to permit an improved adherence thanks to the wraps of helical braid of fibers that create a continuous embossed rib placed on bar bearing core (Fig. 1a and b), composed by a basalt fiber filament rowing. The nominal diameter of rods, provided by manufacturer is of 4 mm. The specimen geometric features have been determined adapting prescriptions provided by Italian Technical Document [21] to a little smaller sample. In particular, for an accurate interpretation of characteristic mechanical values derived by following tests, the rod equivalent cross section (A_b), that results equal to 9.89 mm^2, has been determined, so the rod equivalent diameter results equal to 3.55 mm. This, can be considered a first, important results: in fact a substantial difference can be observed between the effective and the declared (4 mm) diameter. The rib pitch, determined adapting prescription addressed to steel rods for concrete [22] is of 8.41 mm.

2.1.2. Laboratory characterization

In order to obtain further information about rods, different laboratory analysis have been performed.

Fourier Transform Infrared spectroscopy (FT-IR analysis) has been performed on small resin samples taken both from the core and from the rib. The analysis has been performed in the attenuated total reflectance mode with an Avatar 330 spectrometer (Thermo Nicolet, Germany). A minimum of 32 scans with a resolution of 4 cm^{-1} has been used. The total fiber content was determined by gravimetric analysis after a calcination of 2 h at 700 °C in an electric furnace (Optolab – FS5). On the powdered residue a chemical analysis has been performed by X-ray fluorescence (XRF, Thermo ARL, Advant'XP). Moreover the powders have been analyzed with a computer-assisted conventional Bragg–Brentano diffractometer using the Ni-filtered Cu Kα monochromatic radiation (λ = 1.5418 Å) (PW3710 Philips) to obtain the mineralogical analysis. The X-ray diffraction (XRD) patterns were collected at room temperature in a 2θ range of 20–80°, with a scanning rate of 0.005°/s and a step size of 0.02°. Finally to evaluate the microstructure and Tex of the rods, polished surfaces have been prepared by vacuum impregnation with low viscosity epoxy resin and observed with a scanning electron microscope (SEM, FEI, Quanta-200).

Table 1
Main features of BFRP rods and BF ropes (by manufacturer).

	Basalt fiber rod features	Basalt fiber yarn features
Filament diameter (μm)	13–20	13
Linear density (tex)	68–4800	1200
Material density (g/cm^3)	2.8	/
Breaking strain (%)	4.5–8	/
Filaments number	/	18
Size	/	Silane
Size quantity (%)	/	0.5–1.0
Water content (%)	/	<0.2%

2.2. BF ropes

2.2.1. Main features

Basalt fibers ropes of 5 mm and 4 mm of nominal diameter (declared by manufacturer), have been used in experimental program. A digital caliper (accuracy of 0.02 mm) was used to measure and verify the correctness of these nominal diameters and a very good agreement was found in this case. The 5 mm rope is obtained braiding eight rows of basalt fiber yarns over an inner core in turn composed by others braided eight rows of basalt fiber yarns (Fig. 2a–c); these structure can be defined hierarchical [23]. The 4 mm rope instead is obtained braiding eight rows of basalt fiber yarns over an only row of basalt fiber yarn. The relevant features of continuous basalt fiber yarn used to create the ropes, provided by manufacturer, are also reported in Table 1.

2.2.2. Laboratory characterization

In order to obtain further information about the physical and chemical properties of the ropes, the basalt fibers have been characterized with the same techniques reported for rods. The fiber density has been determined by a picnometer (Accupic 1330 apparatus, Micromeritics, Norcross, GA, USA).

2.3. Tensile test

2.3.1. Specimen preparation

Previous research [19,20] and preliminary tests have indicated that direct pulling of rods and ropes is a very difficult task by using a common tensile testing machine, and have shown the need of an anchoring system. Design and production of anchorage is very important for reliability of test results because a wrong anchor alignment could cause undesired failure modes. Following the procedure proposed by [19,20] an anchorage system consisting of a steel pipe filled with a tixotropic epoxy resin (Fig. 3) has been proposed for rods. Based on preliminary tests, it was determined that anchors of 150 mm could offer adequate restraint. The dimension of the specimens have been derived according to [21]: a total specimen length greater than $40d_b$ plus $2l_a$ is provided as recommended, let it be d_b the diameter of the bar and l_a the anchorage length. Plastic caps equipped with holes lightly larger than the bars diameter have been used to close the ends of the pipes and to keep the bar in the center of the pipe (Fig. 4a and b). A wooden formwork has been used to keep the bar and the pipe vertically aligned during the resin setting, and the specimen ends have been handled one step at a time. After 24 h the epoxy resin was hardened so that the specimen could be turned and the second end prepared. During this period the values of temperature and relative humidity could be assumed as constant. As regards ropes, the dimensions of the specimens have been derived by recommendation for similar products as steel spun or generic fiber ropes contained in [24,25]. The test piece shall be of adequate length to give an effective length (L_u) between terminations set by these standards. In particular, following [24], for ropes with a diameter lower than 6 mm, the minimum length between machine chucks has to be greater than 300 mm, while following [25] the minimum length between machine chucks has to be greater than 400 mm. This system has been made by a steel pipe filled with an epoxy resin, so the specimens, with a total length (L_p) of 700 mm, are provided with two anchoring system (one for every end), with a length (L_a) of 100 mm, leaving an effective length (L_u) of 500 mm. The steel pipes have been threaded and steel threaded caps have been used to close the ends of the pipes and to keep the rope in the center of the pipe (Fig. 5). For this purpose, the rope has been fixed in the center of the caps before closing the pipe with this. Then the pipe has been filled with epoxy resin using the carefulness to preserve the specimen in vertical position (it has been enough to hang the specimen during this phase) and, also in this case, the specimen ends have been handled one step at a time. After 24 h the epoxy resin was hardened so that the specimen could be turned and the second end prepared.

2.3.2. Tensile test parameters

Five rod specimens have been prepared at the same time and tested together. As regards ropes, ten specimens have been prepared at the same time and in the same climatic conditions and have been divided into two groups (five of 4 mm diameter

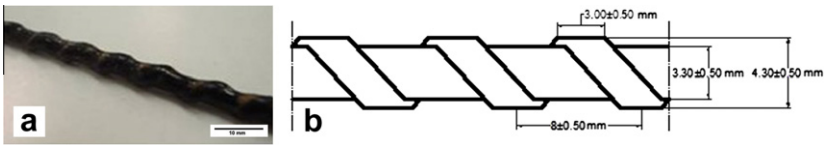

Fig. 1. BFRP rods: photo (a) and direct metric survey (b).

Fig. 2. Five millimeter diameter basalt fibers rope and its structure.

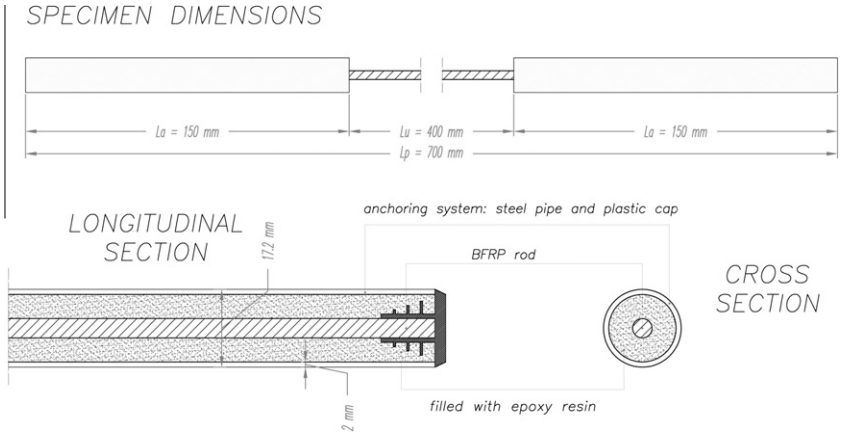

Fig. 3. BFRP rods specimen dimensions and details of anchoring system.

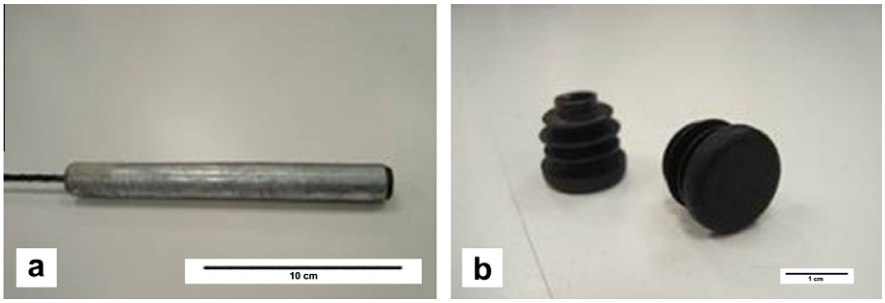

Fig. 4. Anchoring system (a) and the plastic caps used (b).

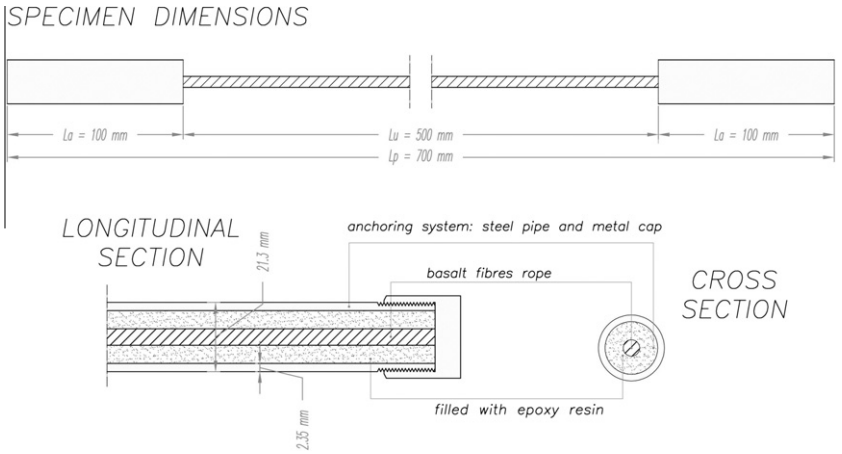

Fig. 5. BF ropes specimen dimensions and details of anchoring system.

and five of 5 mm). An universal testing machine by Zwick/Roell has been used for the tests. The top end of the specimen has been first fixed on the top jaw of the machine, and then also the bottom end has been fixed before applying the load. The load has been applied at a constant speed of 25 N/s until the failure of the specimen. It is notably that rod specimens rupture occurred in a time included between one and 10 min, according to [21] prescriptions. For all the specimens breaking force (F_{fu}) and breaking elongation (ΔL_{Ffu}) have been recorded. As regards ropes, to check if the anchoring system could affect the test, also the place on the sample where the break occurs has been recorded. In particular, as suggested by [24], if the distance between rupture point and anchoring steel pipe has been greater than two times the diameter of the rope, the failure mode has been considered satisfactory and the test has been accepted.

3. Test results and discussion

3.1. Laboratory characterization of rods and ropes

The physical characteristics of the rods are summarized in Table 2. The obtained results are in good agreement with the information reported in technical sheet. In particular they confirmed that the rods are obtained with a single resin that can be classified as vinyl ester. No differences have been found by FTIR analysis between the core and the rib matrix. The fiber content, evaluated by thermogravimetric analysis, is almost 84%. Fig. 6 reports the SEM images of a rod cross section with which, using image analysis software, filament average diameter and core and rib average filament number have been determined (Table 2). Moreover the images show that the resin properly wets the fibers creating a strong fiber/matrix interface. Damage at fiber level are also visible probably due to cutting step for the SEM analysis.

Table 2
Main features of BFRP rods and BF ropes (by laboratory analysis).

	Basalt fiber rod features	Basalt fiber rope features
Filament average diameter (μm)	16.50 (S.D.: 2.54)	13.00 (S.D.: 1.76)
Core average filaments number	23,000	/
Rib average filaments number	5700	/
Resin	Vinylester	/
Size	/	None
Ribs pitch (mm)	8.41	/
Equivalent diameter (mm)	3.55	/
Fiber content (wt.%)	83.77	/
Equivalent cross section (mm^2)	9.89	/
Fiber density (g/cm^3)	/	3.999 ± 0.005
Tow average filaments number	/	6500
5 mm tow number	/	16
4 mm tow number	/	9

Regarding the fiber chemical analysis, Table 3 reports the results obtained on both the fiber from BFRP rods (extracted after calcination step) and RP ropes. The results are consistent with the typical composition of basalt. In particular, having silica content higher than 46 wt.%, it can be classified as acidic basalt [26] with 10 wt.% of iron oxide that justifies the dark color. The slight differences between the chemical composition of basalt in the rods and in the ropes are consistent with a natural material. The mineralogical analysis is consistent, in both samples, with that of an amorphous material. Finally, in Fig. 7, the SEM images of fibers cross section are reported. Using image analysis software, filament average diameter and average filament number have been determined (Table 2). The data underline that the diameter distribution is quite narrow and centered at around 13 μm.

3.2. BFRP rods

All of the specimens failed suddenly with the same failure mode, showing a linear behavior until a fragile rupture (Fig. 8), in fact no post yield zone has been observed, for each graph, this being in agreement with results obtained by other researchers [27] for GFRP and BFRP rods. The values of breaking force (F_{fu}) and breaking elongation (ΔL_{Ffu}) are provided by test machine while breaking stress f_u, elastic modulus E_f, and breaking strain ε_{fu}, are defined using, respectively, Eqs. (1)–(3), proposed by [21]:

$$f_u = F_{fu}/A_b \quad (1)$$

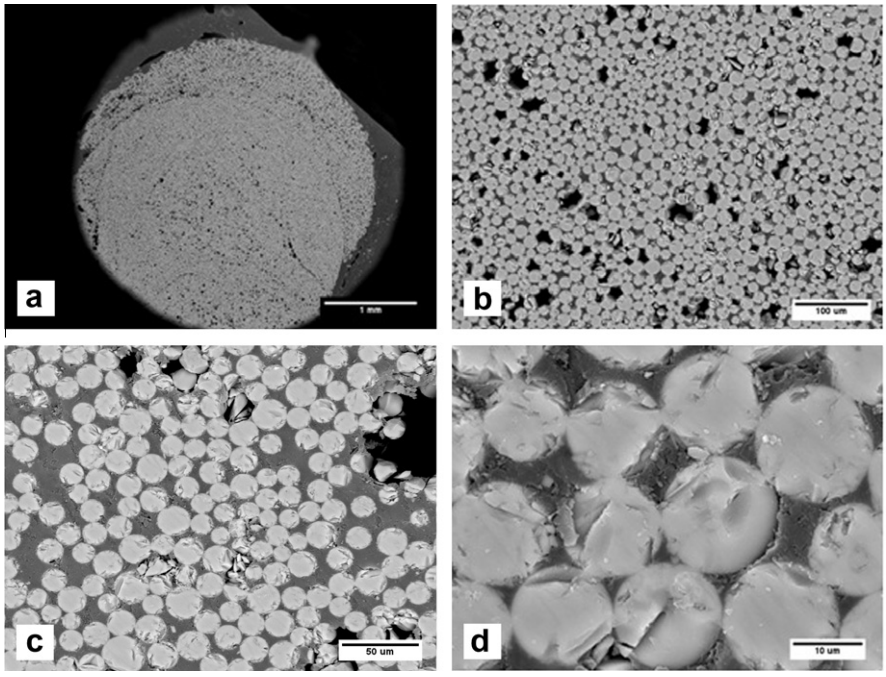

Fig. 6. SEM images of BFRP rod (back-scattered electrons image): cross section (a), consecutive zooms (b–d) needed to determine, using image analysis software, average filament number and filament diameter. It is possible to note that the resin properly wets the fibers creating a strong fiber/matrix interface. Damage at fiber level are also visible probably due to cutting step for the SEM analysis.

Table 3
Basalt fiber chemical composition obtained by XRF.

Oxides (wt.%)	Fiber from BFRP rods	Fiber from BF ropes	Oxides (wt.%)	Fiber from BFRP rods	Fiber from BF ropes
SiO_2	50.9	50.48	TiO_2	1.44	0.94
Al_2O_3	18.3	16.69	SrO	0.05	0.11
CaO	8.94	7.59	ZnO	0.15	0.02
MgO	3.61	5.93	P_2O_5	0.18	0.3
Na_2O	3.53	4.53	MnO	0.03	0.13
K_2O	1.94	2.66	Cr_2O_3	0.01	0.03
Fe_2O_3	10.7	10.2	NiO	0.05	0.03

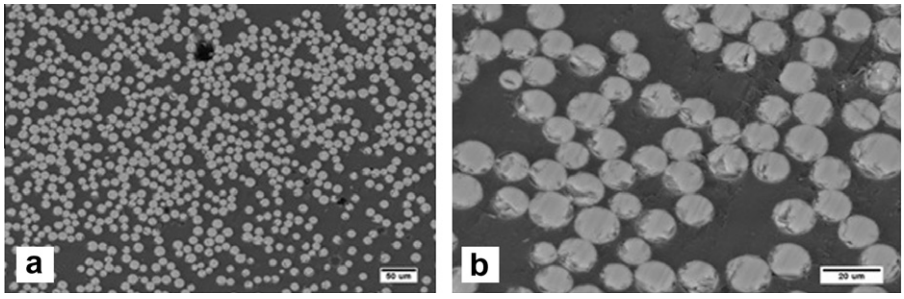

Fig. 7. SEM images of basalt fiber rope (back-scattered electrons image): cross section (a), particular of fibers (b).

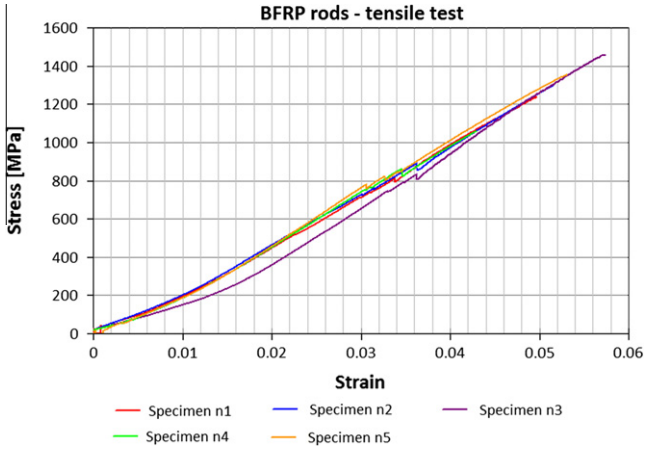

Fig. 8. Graph of stress–strain curve.

$$E_f = (F_1 - F_2)/(\varepsilon_1 - \varepsilon_2) \cdot A_b \quad (2)$$

$$\varepsilon_{fu} = F_{fu}/E_f \cdot A_b \quad (3)$$

where A_b is the rod equivalent cross section (equal to 9.89 mm^2, as reported in Section 2.1.1); F_1, ε_1 are respectively the force and the strain corresponding to the 50% of breaking stress, while F_2, ε_2 are the force and the strain corresponding to the 20% of breaking stress. The average values and standard deviations are reported in Table 4. The only comparison with technical sheet values can be made about "breaking strain" and the obtained results are in good agreement with the information provided by manufacturer. Table 5 presents a comparison between the values obtained from tensile tests and the ones of similar products (STEEL, GFRP, CFRP, and AFRP rods) used in construction field, available in literature [20,27–29]. The main purpose of the study has been the tensile characterization of basalt FRP (BFRP) rods, but Table 6 reports the reference values [7,11,30] for continuous basalt fibers in others employments to show the influence of matrix and product technological features, and it is clear like filament, fabric or fibers tow, could offer different performances from the ones exhibited by rods tested in this work.

3.3. BF ropes

All specimens failed suddenly, with a fragile behavior and with the same failure mode. The failure starts from the external yarns of the rope with an immediate decrease of the applied force. Then the load was transferred to the internal ones that offered another small resistance reserve but failed in no time and the excessive decrease of the applied force determined the stop of the test by the testing machine. The failure mode of 5 mm diameter specimens is shown in Fig. 9. The place on the test piece where the break occurs can be considered satisfactory in every case. The values of breaking force (F_{max}), breaking elongation (ΔL_{Fmax}), provided by test machine, the average value and standard deviation of them are reported in Table 7, for 5 mm diameter specimens, and in Table 8 for the 4 mm ones (the test on specimen n.9 cannot be considered for the purpose of this work for the failure of the anchoring system placed in one end of the specimen, caused by a resin application fault, as can be seen in Fig. 10a and b). Moreover, also breaking strain (ε_{max}) referred to free length (L_u) and breaking stress (σ_{max}) related to the nominal cross section of the rope, assuming that remain constant during the test, have been reported. As regards the relationship between force and elongation, it is interesting to note that in 5 mm specimens this entities are bind by a non-linear law, almost exactly parabolic, that shows an increase of stiffness nearing the rupture point (Fig. 11). In 4 mm diameter ropes, the unique structure of the rope is subjected to several small damages during the test, that cause a force–elongation curve trend not so regular, but showing an increase of stiffness too (Fig. 12). It is fair to presume that this behavior, very similar to the one noticed also on steel wire ropes [31], is due to the morphology of the rope and at the disposition of the yarns inside it. In fact previous works [11,32] show that single basalt fiber filament subject to tensile stress responds with a linear trend of stress–strain curve and with an elastic-fragile behavior. The analytical law used to round off the force–elongation trend of the rope, is the one of a parable intersecting the origin of the Cartesian plane. The equations of this relationship obtained using a commercial spreadsheet are reported in Tables 9 and 10 with

Table 4
Tensile tests results.

Specimen number	Breaking elongation ΔL_{Ffu} (mm)	S.D.	Breaking force F_{fu} (N)	S.D.	Breaking stress f_{fu} (MPa)	S.D.	Elastic modulus E_f (GPa)	S.D.	Breaking strain ε_{fu}	S.D.
1	19.88		12,260		1240		26.25		0.047	
2	20.63		12,836		1298		26.87		0.048	
3	22.96		14,447		1461		29.21		0.050	
4	17.16		10,469		1059		27.53		0.038	
5	21.21		13,382		1353		29.68		0.046	
Average values	20.37	1.90	12,679	1319	1282	133	27.91	1.33	0.046	0.004

Table 5
Comparison between tensile tests results and reference values.

	STEEL[a]	GFRP[a]	GFRP[b]	GFRP[c]	GFRP[c]	GFRP[d]	CFRP[a]	CFRP[b]	AFRP[b]	BFRP[d]	BFRP
Nominal yield stress (MPa)	276–517	–	–	–	–	–	–	–	–	–	–
Tensile strength (MPa)	482–689	482–1585	770	824.5	760	918	600–3688	2250	1724–2537	707	1282
Elastic Modulus (GPa)	200	35–51	37	50	40	35.2	103–579	147	41–125	24.8	27.91
Yeld strain (%)	1.4–2.5	–	–	–	–	–	–	–	–	–	–
Ultimate strain (%)	6–12	1.2–3.1	2.1	1.78	1.85	2.69	0.5–1.9	1.5	1.9–4.4	3.03	4.6

[a] Values from [20].
[b] Values from [28].
[c] Values from [29].
[d] Values from [27].

Table 6
Basalt fiber reference values.

	Basalt fiber[a] (filament)	Basalt fiber[b] (fabric sheet)	Basalt fiber[c] (2400 fibers tow)	Basalt fiber rods
Tensile strength (MPa)	992	2332	2600	1282
Elastic modulus (GPa)	76	91	90	27.91
Ultimate strain (%)	2.56	2.56	3.1	4.6

[a] Values measured by [11].
[b] Values measured by [30].
[c] Values measured by [7].

Fig. 9. Specimens after the tensile test.

the relative value of coefficient R^2 that shows how better the analytical relation round off the experimental curve. It is relevant the fact that the 5 mm BF rope shows an average breaking force that is almost twice that of the 4 mm one. This could be easy explained by the fact that, the 5 mm rope has a filaments number (and so an effective working cross section) that is almost twice than of the 4 mm one. This indicates that the rope's structure is able to arrange a good collaboration between filaments and so the number of these determines the rope performance. Moreover, the test results legitimate to think that stiffness and deformability are affected by filaments number: in fact, the average values breaking elongation is greater for 4 mm diameter rope than 5 mm diameter while the force–elongation curve shows the stiffness difference between

Table 7
Tensile test results on 5 mm diameter specimens.

Specimen number	Nominal diameter (mm)	Breaking elongation ΔL_{Fmax} (mm)	S.D.	Breaking force F_{max} (N)	S.D.	Breaking strain ε_{max}	S.D.	Breaking stress σ_{max} (MPa)	S.D.
1	5	20.83		6478.93		0.042		330.14	
2	5	19.99		6977.13		0.040		355.52	
3	5	18.86		6438.05		0.038		328.05	
4	5	18.77		6480.70		0.038		330.23	
5	5	18.58		6781.09		0.037		345.53	
Average values		19.40	0.87	6631.18	212.26	0.039	0.002	337.89	10.82

Table 8
Tensile test results on 4 mm diameter specimens.

Specimen number	Nominal diameter (mm)	Breaking elongation ΔL_{Fmax} (mm)	S.D.	Breaking force F_{max} (N)	S.D.	Breaking strain ε_{max}	S.D.	Breaking stress σ_{max} (MPa)	S.D.
6	4	27.52		3404.46		0.055		271.06	
7	4	28.77		3463.54		0.057		275.76	
8	4	24.50		3200.37		0.049		254.81	
9	4	–		–		–		–	
10	4	16.77		2560.72		0.033		203.88	
Average values		24.39	4.67	3157.27	357.99	0.05	0.009	251.38	28.50

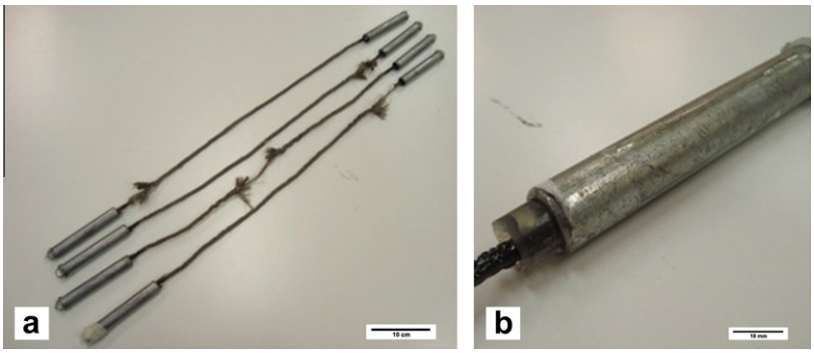

Fig. 10. Specimens after the tensile test (a) and the specimen n.9 anchoring system failure (b).

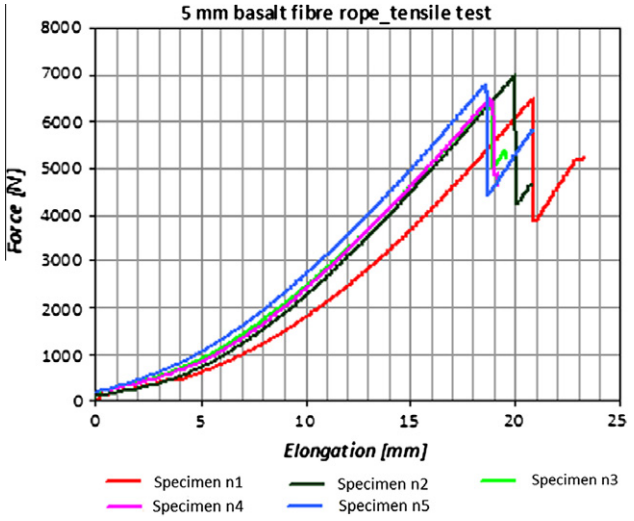

Fig. 11. Five millimeter rope: Force–Elongation graph.

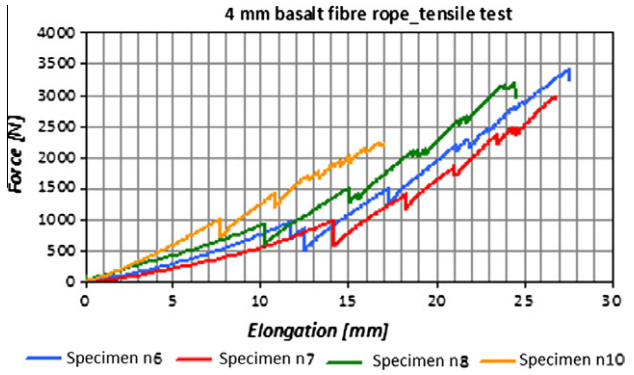

Fig. 12. Four millimeter rope: Force–Elongation graph.

Table 9
Relationship between force and elongation in 5 mm diameter BF rope.

Specimen number	Relationship	R^2
1	$F = 12.084\ \Delta L^2 + 62.234\ \Delta L$	0.999
2	$F = 13.248\ \Delta L^2 + 93.892\ \Delta L$	0.999
3	$F = 11.526\ \Delta L^2 + 131.2\ \Delta L$	0.999
4	$F = 12.429\ \Delta L^2 + 116.53\ \Delta L$	0.998
5	$F = 11.25\ \Delta L^2 + 159.68\ \Delta L$	0.999

Table 10
Relationship between force and elongation in 4 mm diameter BF rope.

Specimen number	Relationship	R^2
6	$F = 3.4521\ \Delta L^2 + 27.265\ \Delta L$	0.985
7	$F = 3.429\ \Delta L^2 + 14.913\ \Delta L$	0.982
8	$F = 3.2507\ \Delta L^2 + 49.682\ \Delta L$	0.990
9	–	–
10	$F = 1.4931\ \Delta L^2 + 108.85\ \Delta L$	0.994

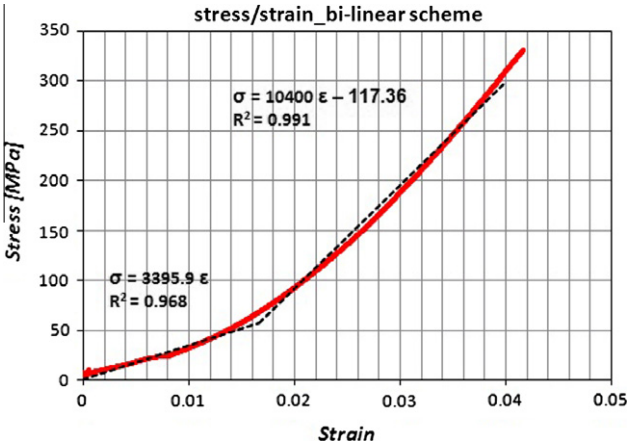

Fig. 13. Graph of bi-linear scheme of stress–strain curve – specimen n.1.

these products. Finally, it has been tried to schematize the parabolic function that describes the mechanical behavior of the ropes through a bi-linear constitutive law in order to have an easier instrument to use in applications (like numerical analysis, for example) that envisaging the employment of basalt fiber ropes. The two branches of the bi-linear law are obtained as the ones that better fit the two part of the stress–strain curve obtaining the highest values of determination coefficient in the two branches. It is not useless underline that breaking stress (σ_{max}) related to the nominal cross section of the rope was obtained assuming that they remain constant during the test. Figs. 13 and 14 resume, as an example, the exposed procedure applied on the specimen n. 1 and 6, while Tables 11 and 12 summarizes all the results of this analysis. In order to understand the effective employments of BF rope, a comparison with other products, for which it could represents a good alternative, is presented in Table 13. BF rope seems to be better than other fibers ropes like canvas and polyester (PES), (that are usually used in marine field) in terms of breaking force but exhibit lower performance compared to steel cables, high density polyethylene (HDPE), polyethylene (PE) or liquid crystal polymer (LCP).

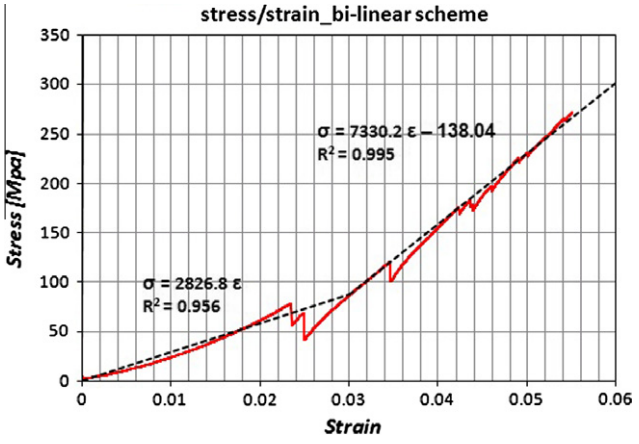

Fig. 14. Graph of bi-linear scheme of stress–strain curve – specimen n.6.

Table 11
Bi-linear constitutive law in 5 mm diameter BF rope.

Specimen number	1st Branch eq.	R^2	2nd Branch eq.	R^2
1	$\sigma = 3395\ \varepsilon$	0.968	$\sigma = 10{,}400\ \varepsilon - 117.36$	0.991
2	$\sigma = 4016.3\ \varepsilon$	0.947	$\sigma = 11{,}628\ \varepsilon - 117.05$	0.997
3	$\sigma = 4896.6\ \varepsilon$	0.965	$\sigma = 11{,}099\ \varepsilon - 95.944$	0.997
4	$\sigma = 4616.4\ \varepsilon$	0.957	$\sigma = 11{,}372\ \varepsilon - 104.37$	0.997
5	$\sigma = 5627\ \varepsilon$	0.976	$\sigma = 11{,}589\ \varepsilon - 92.74$	0.997

Table 12
Bi-linear constitutive law in 4 mm diameter BF rope.

Specimen number	1st branch eq.	R^2	2nd branch eq.	R^2
6	$\sigma = 2826.8\ \varepsilon$	0.956	$\sigma = 7330.2\varepsilon - 138.04$	0.995
7	$\sigma = 2164.2\ \varepsilon$	0.956	$\sigma = 6374.4\varepsilon - 119.16$	0.966
8	$\sigma = 3286\ \varepsilon$	0.955	$\sigma = 7257\varepsilon - 104.83$	0.983
9	–	–	–	–
10	$\sigma = 4867.3\ \varepsilon$	0.982	$\sigma = 5362.1\varepsilon - 3.67$	0.966

Table 13
Comparison between basalt and other fiber rope (5 mm diameter).

	Canvas fiber[a]	Steel spun[b]	HDPE fiber[c]	PES fiber[c]	LCP fiber[c]	PE fiber[c]	Basalt fiber
Breaking force F_{max} (N)	1600	4900–23,000	21,000	3300–4800	11,500	1500–4000	6631

[a] Values from [33].
[b] Values from [34].
[c] Values from [35].

4. Conclusion

In this paper an experimental work with the aim of validate a test protocol for tensile characterization of BFRP rods and proposing a new one for BF ropes is presented.

The protocol previously used by other researcher [19,20] for the test on other GFRP and CFRP rods, in fact, rises to be efficient also for BFRP rods. The comparison between experimental results and the ones of other similar products shows that BFRP rods could be a good alternative to other FRP rods. The tested BFRP rods seems to be not so rigid (less than glass FRP rods) but rather deformable and with good tensile strength (better than GFRP rods). The performances showed by this innovative product could suggest several employment in several fields and in particular it seems to be suitable for repointing application, in strengthening and restoration of historical masonries. Anyway, particular attention could be paid by designers in checking and verifying technical data provided by manufacturer: in fact not all of these data are in agree with product real features (for example, diameter declared is different than effective one). Do not consider this fact should have negative implication on construction safety.

As regards BF ropes, the proposed test protocol seems to be efficient in order to have a tensile characterization of this product. Experimental results confirm that BF ropes have good mechanical performances. This has suggested their possible employment for strengthening purposes. In particular, an innovative technique, aimed to strengthen regular, irregular and poor masonry through continuous basalt ropes, has been still being tested in our laboratories and on site [36]. The first results are encouraging, and they will be presented as soon as possible.

Nevertheless, it is important to underline that durability tests are needed before extensively applying basalt products. While basalt, as a material, in fact, have a good durability, it is necessary a better investigation in order to verify basalt products durability and this surely represent a future development of this work. In this way, accelerated ageing tests are currently under way.

References

[1] Militky J et al. Influence of thermal treatment on tensile failure of basalt fibers. Eng Fract Mech 2002;69:1025–33.
[2] Militký J et al. Mechanical properties of basalt filaments. Fibres Text East Eur 2007;15(5–6):64–5.
[3] Fahmy MFM, Wu Z. Evaluating and proposing models of circular concrete columns confined with different FRP composites. Compos: Part B 2010;41:199–213.
[4] Wei B et al. Surface modification and characterization of basalt fibers with hybrid sizings. Compos: Part A 2011;42:22–9.
[5] Park JM et al. A study of interfacial aspects of epoxy-based composites reinforced with dual basalt and SiC fibres by means of the fragmentation and acoustic emission techniques. Compos Sci Technol 1999;59:355–70.
[6] Morozov NN et al. Material based on basalts from the European North of Russia. Glass Ceram 2001;58:100–4.
[7] Wei B et al. Environmental resistance and mechanical performance of basalt and glass fibers. Mater Sci Eng A 2010;527:4708–15.
[8] Wei B et al. Degradation of basalt fibre and glass fibre/epoxy resin composites in seawater. Corros Sci 2011;53:426–31.
[9] Fiore V et al. Glass–basalt/epoxy hybrid composites for marine applications. Mater Des 2011;32:2091–9.
[10] Carmisciano S et al. Basalt woven fiber reinforced vinylester composites: flexural and electrical properties. Mater Des 2011;32:337–42.
[11] Sim J et al. Characteristics of basalt fiber as a strengthening material for concrete structures. Compos: Part B 2005;36:504–12.
[12] Papanicolaou C et al. Externally bonded grids as strengthening and seismic retrofitting materials of masonry panels. Constr Build Mater 2011;25:504–14.

[13] Brik VB. Advanced concept concrete using basalt fiber composite reinforcement. Final report for Highway-IDEA Project 86 submitted to NCHRP-IDEA; 2003.
[14] Landucci G et al. Design and testing of innovative materials for passive fire protection. Fire Saf J 2009;44:1103–9.
[15] Scheffler C et al. Aging of alkali-resistant glass and basalt fibers in alkaline solutions: Evaluation of the failure stress by Weibull distribution function. J Non-Cryst Solids 2009;355:2588–95.
[16] Kogan FM, Nikitina OV. Solubility of chrysotile asbestos and basalt fibers in relation to their fibrogenic and carcinogenic action, Workshop on biopersistence of respirable synthetic fibers and minerals held, Lyon, France; 1992.
[17] Valluzzi MR et al. Mechanical behaviour of historic masonry structures strengthened by bed joints structural repointing. Constr Build Mater 2005;19: 63–73.
[18] Tinazzi D et al. FRP-structural repointing of masonry assemblages. In: Humar J, Razaqpur AG. editors. Proc, 3rd inter conf on advanced composite materials in bridges and structures. Ottawa, Canada; 2000. p. 585–92.
[19] Micelli F, Nanni A. Tensile characterization of FRP rods for reinforced concrete structures. Mech Compos Mater 2003;39:293–304.
[20] Kocaoz S et al. Tensile characterization of glass FRP bars. Compos: Part B 2005;36:127–34.
[21] CNR DT 203/2006: Istruzioni per la progettazione, l'esecuzione ed il controllo di strutture di calcestruzzo armato con barre di materiale composito fibrorinforzato.
[22] UNI EN 15630-1: Steel for the reinforcement and pre-stressing concrete – Test methods – Part 1: Reinforcing bars, wire rod and wire; 2010.
[23] Leech CM. The modelling of friction in polymer fibre ropes. Int J Mech Sci 2002;44:621–43.
[24] UNI 3171: Steel wire ropes for general purposes – Determination of actual breaking load; 1985.
[25] UNI EN ISO 2307: Fibre ropes – Determination of certain physical and mechanical properties; 2005.
[26] Le Maitre RW. The chemical variability of some common igneous Rocks. J Petrol 1976;17:589–98.
[27] Reyes-Araiza JL et al. Comparative study on tensile behavior of inorganic fibers embedded in unsaturated polyester bisphenol "A" – styrene copolymer. Inorg Mater 2008;44:549–54.
[28] Gravina RJ, Smith ST. Flexural behaviour of indeterminate concrete beams reinforced with FRP bars. Eng Struct 2008;30:2370–80.
[29] Galati N et al. Strengthening with FRP bars of URM walls subject to out-of-plane loads. Constr Build Mater 2006;20:101–10.
[30] Wu Z et al. Tensile fatigue behaviour of FRP and hybrid FRP sheets. Compos: Part B 2010;41:396–402.
[31] Feyrer K. Wire ropes. Tension, endurance, reliability. Berlin: Springer Verlag; 2000.
[32] Zhu L et al. Constitutive equations of basalt filament tows under quasi-static and high strain rate tension. Mater Sci Eng A 2010;527:3245–52.
[33] Monteisola Corde s.n.c. <http://www.corde.it> [accessed 31.03.11].
[34] Funi 90 s.rl. <http://www.funi90.it> [accessed 31.03.11].
[35] Treccificio Borri s.n.c <http://www.treccificioborri.it> [accessed 31.03.11].
[36] Italian Patent application n. BO2011A000327 "Metodo per rinforzare opere edili ed opere rinforzate così ottenute" (Method for reinforcing building works and building works reinforced by this method"), [registered 07.06.11].